

COVID-19-like symptoms observed in Chinese tree shrews infected with SARS-CoV-2

Ling Xu^{1,2,#}, Dan-Dan Yu^{1,2,#}, Yu-Hua Ma³, Yu-Lin Yao^{1,4}, Rong-Hua Luo^{1,2}, Xiao-Li Feng², Hou-Rong Cai⁵, Jian-Bao Han², Xue-Hui Wang^{1,4}, Ming-Hua Li², Chang-Wen Ke⁶, Yong-Tang Zheng^{1,2,3,*}, Yong-Gang Yao^{1,3,4,7,*}

¹ Key Laboratory of Animal Models and Human Disease Mechanisms of the Chinese Academy of Sciences, KIZ-CUHK Joint Laboratory of Bioresources and Molecular Research in Common Diseases, Kunming Institute of Zoology, Chinese Academy of Sciences, Kunming, Yunnan 650223, China

² Kunming National High-level Biosafety Research Center for Non-Human Primates, Center for Biosafety Mega-Science, Kunming Institute of Zoology, Chinese Academic of Sciences, Kunming, Yunnan 650107, China

³ National Resource Center for Non-Human Primates, National Research Facility for Phenotypic & Genetic Analysis of Model Animals (Primate Facility), Kunming Institute of Zoology, Chinese Academy of Sciences, Kunming, Yunnan 650107, China

⁴ Kunming College of Life Science, University of Chinese Academy of Sciences, Kunming, Yunnan 650204, China

⁵ Department of Respiratory and Critical Care Medicine, the Affiliated Drum Tower Hospital of Nanjing University, Nanjing, Jiangsu 210008, China

⁶ Medical Key Laboratory for Repository and Application of Pathogenic Microbiology, Guangdong Provincial Center for Disease Control and Prevention, Guangzhou, Guangdong 510440, China

⁷ CAS Center for Excellence in Brain Science and Intelligence Technology, Chinese Academy of Sciences, Shanghai 200031, China

ABSTRACT

The coronavirus disease 2019 (COVID-19) pandemic continues to pose a global threat to the human population. Identifying animal species susceptible to infection with the SARS-CoV-2/HCoV-19 pathogen is essential for controlling the outbreak and for testing valid prophylactics or therapeutics based on animal model studies. Here, different aged Chinese tree shrews (adult group, 1 year old; old group, 5–6 years old), which are close relatives to primates, were infected with SARS-CoV-2. X-ray, viral shedding, laboratory, and histological analyses were performed on different days post-inoculation (dpi). Results showed that Chinese tree

shrews could be infected by SARS-CoV-2. Lung infiltrates were visible in X-ray radiographs in most infected animals. Viral RNA was consistently detected in lung tissues from infected animals at 3, 5, and 7 dpi, along with alterations in related parameters from routine blood tests and serum biochemistry, including increased levels of aspartate aminotransferase (AST) and blood urea nitrogen (BUN). Histological analysis of lung tissues from animals at 3 dpi (adult group) and 7 dpi (old group) showed thickened alveolar septa and interstitial

Received: 15 July 2020; Accepted: 21 July 2020; Online: 21 July 2020
Foundation items: This work was partly supported by the National Key R&D Program of China (2020YFC0842000 to Y.T.Z.), National Natural Science Foundation of China (U1902215 to Y.G.Y.), National Science and Technology Major Projects of Infectious Disease Funds (2017ZX10304402 to Y.T.Z.), Yunnan Province (2018FB046 to D.D.Y.), and CAS “Light of West China” Program (xbzg-zdsys-201909 to Y.G.Y. and Y.T.Z.)

*Authors contributed equally to this work

*Corresponding authors, E-mail: zhengyt@mail.kiz.ac.cn; yaoyg@mail.kiz.ac.cn

DOI: 10.24272/j.issn.2095-8137.2020.053

Open Access

This is an open-access article distributed under the terms of the Creative Commons Attribution Non-Commercial License (<http://creativecommons.org/licenses/by-nc/4.0/>), which permits unrestricted non-commercial use, distribution, and reproduction in any medium, provided the original work is properly cited.

Copyright ©2020 Editorial Office of Zoological Research, Kunming Institute of Zoology, Chinese Academy of Sciences

hemorrhage. Several differences were found between the two different aged groups in regard to viral shedding peak. Our results indicate that Chinese tree shrews have the potential to be used as animal models for SARS-CoV-2 infection.

Keywords: SARS-CoV-2/HCoV-19; Treeshrews; Animal model; Susceptibility; COVID-19

INTRODUCTION

The coronavirus disease 2019 (COVID-19) pandemic, which is caused by infection with a novel human coronavirus (SARS-CoV-2/HCoV-19/2019-nCoV) (Lu et al., 2020a; Wu et al., 2020; Zhou et al., 2020b; Zhu et al., 2020), continues to exhibit widespread and intense global transmission. As of 08 July 2020, COVID-19 has caused over 539 906 deaths and 11 669 259 cases in 216 countries, areas, or territories (<https://www.who.int/emergencies/diseases/novel-coronavirus-2019>), with numbers still increasing. Based on recently available evidence, SARS-CoV-2 is considered to have a zoonotic origin (Wong et al., 2020), with bats and pangolins being the most probable natural reservoirs and intermediate hosts, respectively (Lam et al., 2020; Xiao et al., 2020; Zhang et al., 2020b; Zhou et al., 2020a; Zhou et al., 2020b). Hitherto, there are no licensed vaccines or prophylactics or therapeutics available to prevent or treat COVID-19, although results from initial clinical observations are promising for convalescent plasma therapy (Duan et al., 2020) and monoclonal antibody (tocilizumab) treatment, which targets the IL-6 pathway to reduce cytokine storm (Xu et al., 2020). Clinical trials for Remdesivir have not yielded statistically significant clinical benefits in patients with severe COVID-19 according to two recent randomized, double-blind, placebo-controlled, multicenter trials (Goldman et al., 2020; Wang et al., 2020c), although controversies regarding the efficacy of Remdesivir remain (Grein et al., 2020). Similarly, clinical trials of hydroxychloroquine and/or azithromycin treatment in COVID-19 patients have shown conflicting results regarding clinical outcomes and adverse effects (Geleris et al., 2020; Lagier et al., 2020; Million et al., 2020; Tang et al., 2020; Yu et al., 2020a). To better understand the pathogenesis of COVID-19 and to hunt for effective drugs and vaccines, proper animal models are urgently needed.

Several recent studies have attempted to establish proper models for SARS-CoV-2 infection using a variety of animals, including human ACE2 transgenic mice (Bao et al., 2020), ferrets (Kim et al., 2020; Shi et al., 2020), golden Syrian hamsters (Chan et al., 2020), and non-human primates (Gao et al., 2020; Lu et al., 2020b; Munster et al., 2020; Rockx et al., 2020; Shan et al., 2020; Yu et al., 2020b). These studies have broadened our knowledge on the infection and interspecies transmission of SARS-CoV-2 in animals, as well as on drugs (Williamson et al., 2020) and vaccines (Gao et al., 2020) with potential efficacy. Chinese tree shrews (*Tupaia belangeri chinensis*), which are widely distributed in Southeast

Asia and South and Southwest China, have a close relationship to non-human primates (Fan et al., 2019). These rat-sized experimental animals have been used extensively in biomedical research (Li et al., 2018; Xiao et al., 2017; Yao, 2017), in particular for viral infections, such as hepatitis B and C (Amako et al., 2010; Wang et al., 2012), avian influenza (Xu et al., 2019), and HSV-1 virus infections (Li et al., 2016). Comparison of angiotensin converting enzyme 2 (ACE2, which serves as the SARS-CoV-2 receptor (Zhou et al., 2020b)) protein sequences shows high sequence identity between humans and tree shrews (up to 81%), suggesting that tree shrews may be susceptible to SARS-CoV-2 infection.

In the current study, we investigated whether Chinese tree shrews can be infected by SARS-CoV-2 and therefore used to create a valid animal model for SARS-CoV-2 infection and COVID-19. Our study found direct evidence that Chinese tree shrews are susceptible to SARS-CoV-2 infection and infected animals display viral shedding, lung lesions, and alterations in blood biochemical indices.

MATERIALS AND METHODS

Animals and ethics statement

Healthy adult tree shrews (adult group, 1 year old, $n=13$, including nine males and four females; old group, 5–6 years old, $n=7$, including three males and four females) were sourced from the Experimental Animal Core Facility of the Kunming Institute of Zoology (KIZ), Chinese Academy of Sciences (CAS). All experiments with live SARS-CoV-2 were performed in the animal biosafety level 3 (ABSL3) facility in KIZ, CAS. The animal studies were performed in accordance with the regulations of the Guide for the Care and Use of Laboratory Animals issued by the Ministry of Science and Technology of China. The Institutional Animal Care and Use Committee of KIZ, CAS, approved all protocols used in this study (Approval No: SMKX-20200301-02).

Virus strain

The SARS-CoV-2 strain 107 was obtained from the Guangdong Provincial Center for Disease Control and Prevention, Guangdong Province, China. The virus was amplified in Vero-E6 cells. Median tissue culture infective dose (TCID₅₀) was used to assess virus infectivity, and titers were calculated by the Reed-Muench method (Reed & Muench, 1938).

Animal experiments and laboratory tests

After anaesthetization with ketamine, we performed clinical examinations for each tree shrew to obtain baseline information. Collection of rectal and throat swabs, X-ray tests, laboratory assessments, routine blood tests (i.e., white blood cell count, including lymphocytes, monocytes, and granulocytes), and serum biochemistry tests (i.e., blood urea nitrogen (BUN), total protein, globulin, albumin, aspartate aminotransferase (AST), alanine aminotransferase (ALT)) were performed. Each animal was then inoculated with a total of 300 μL (1×10^7 TCID₅₀) of SARS-CoV-2 by oral (240 μL),

intranasal (20 μ L per nostril), and ocular (10 μ L per eye) routes. The animals were randomly selected at the indicated days post-inoculation (dpi) for clinical examination after anaesthetization (Figure 1). Briefly, throat and anal swabs were added to 1 mL DMEM medium (Gibco, USA) at various time points (adult group: 3, 5, 7, and 14 dpi; old group: 3, 5, 7 and 11 dpi), after which the animals received chest X-ray tests. Blood samples were collected from each animal for routine blood tests and serum biochemistry before euthanasia. Necropsies were then performed to test viral loads and pathological lesions in different tissues, with seven lung lobes, conjunctiva, kidney, urinary bladder, small intestines (duodenum, jejunum, ileum), testes, and ovaries collected for viral RNA detection. We performed hematoxylin and eosin (H&E) staining of lung tissues, which were fixed in 4% paraformaldehyde and embedded in paraffin for further processing. Double-blind assessment of tissue sections was conducted by a pathologist, who scored the tissues for alveolar edema, interstitial edema, hemorrhage, and inflammatory infiltration. Slides were viewed using a Leica microscope (Leica, Germany) with Leica application suite 4.9 software to capture images. The immunofluorescence process was described in our previous study (Zhang et al., 2019). In brief, the sections were deparaffinized in xylene and rehydrated through a graded ethanol series; for antigen retrieval, sections immersed in saline sodium citrate buffer

were microwave heated for 6 min three times. This was followed by cooling to room temperature, washing with 1 \times phosphate-buffered saline (PBS) containing 0.05% Tween-20 (1 \times PBST), and blocked with 10% bovine serum albumin (BSA) at 37 $^{\circ}$ C for 60 min. Anti-SARS-CoV-2 nucleoprotein (NP) (1:200; 40143-R019, Sino Biological, USA) was diluted in BSA and incubated overnight at 4 $^{\circ}$ C. The sections were then washed, and immunoreactivity was detected using FITC-conjugated secondary antibody (1:500; KPL, 172-1506; incubation for 1 h at room temperature). The sections were directly counterstained with 5 μ g/mL 4', 6-diamidino-2-phenylindole (DAPI) for 5 min at room temperature and washed with 1 \times PBST three times. Slides were visualized under an Olympus FluoView 1000 confocal microscope (Olympus, Japan).

Quantitative real-time RT-PCR (qRT-PCR) to detect SARS-CoV-2 RNA

Total RNA was extracted from swabs and serum samples using a High Pure Viral RNA Kit (Roche, Germany) in accordance with the manufacturer's instructions. TRIzol Reagent (Thermo, USA) was applied for RNA isolation using homogenized tissues. We followed the manufacturer's protocols for one-step RT-PCR using a THUNDERBIRD Probe One-Step qRT-PCR Kit (TOYOBO, Japan) to detect SARS-CoV-2 RNA. Previously reported primers targeting the N protein were used, including (5'-GGGAACTTCTCTCTG

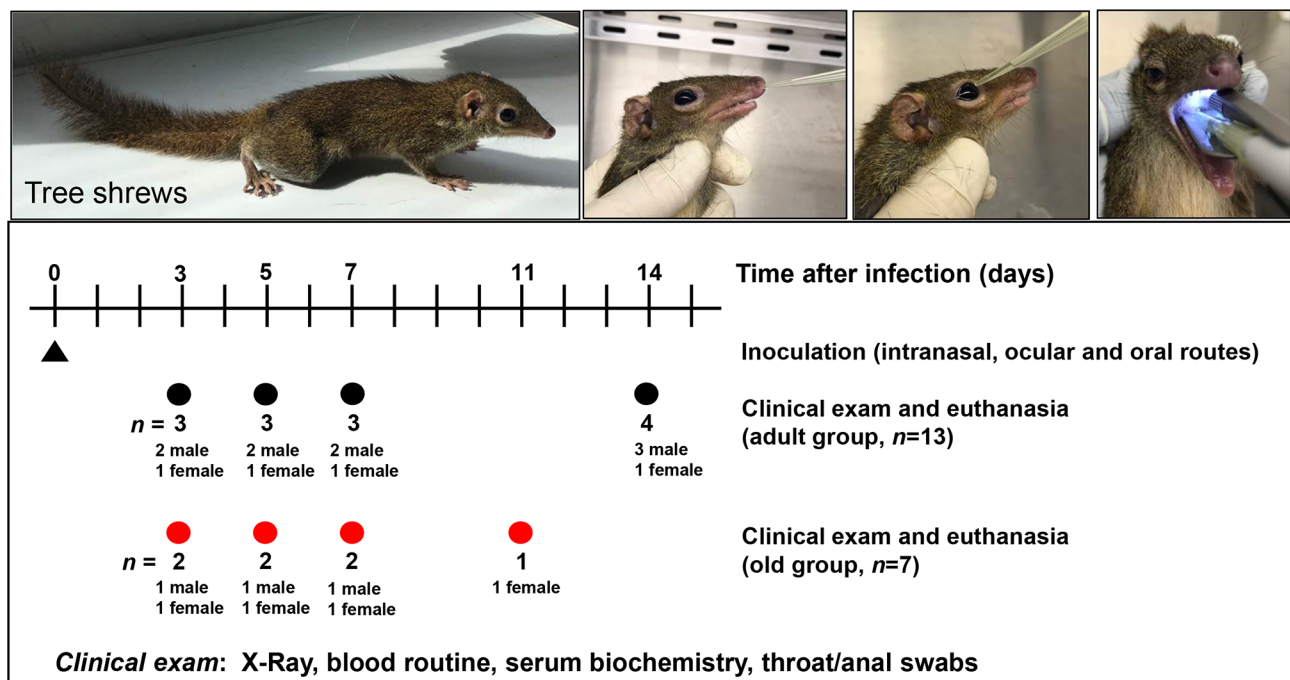


Figure 1 Schematic of experimental design

Tree shrews were divided into two groups, i.e., adult group (n=13, black circles) and old group (n=7, red circles), and inoculated with SARS-CoV-2 (black triangle) via intranasal, ocular, and oral routes. At 0, 3, 5, 7, 11 (old group), or 14 (adult group) days post-inoculation (dpi), clinical examinations were performed to show tree shrew status. Animals from each group were euthanized and necropsied at indicated dpi for virological and pathological assays.

CTAGAAT-3'/5'-CAGACATTTTGCTCTCAAGCTG-3') and probe FAM-TTGCTGCTGCTTGACAGATT-TAMRA-3' (Wang et al., 2020a). In each run, serial dilutions of the SARS-CoV-2 RNA reference standard (National Institute of Metrology, China) were used in parallel to calculate copy numbers in each sample.

Statistical analysis

Comparisons between different groups were conducted using two-tailed Student's *t* test (GraphPad Prism v7). The data are presented as means±standard deviation (*SD*). A *P*-value of <0.05 was considered statistically significant.

RESULTS

In total, 13 adult tree shrews (~1 year old) and seven old tree shrews (5–6 years old) were used for this study. Each animal

was inoculated with SARS-CoV-2 strain 107 (total 300 μ L (1×10^7 TCID₅₀)) by oral (240 μ L), intranasal (20 μ L per nostril), and ocular (10 μ L per eye) routes (Figure 1). After inoculation with SARS-CoV-2, tree shrews were randomly selected on a specific schedule for X-ray, routine blood work and serum biochemistry tests (Figure 1). Selected tree shrews were euthanized for necropsy and examination of pathological changes at indicated time points. As shown in Figure 2, lung infiltrates became visible on the X-rays from 3 dpi and were sustained to 14 dpi (adult group) or 11 dpi (old group). We used different sampling times for the adult and old groups at the last time point (14 dpi vs. 11 dpi) simply because the old animals refused to eat and drink due to stress during the experiments. Most infected animals (17/20, 85%) presented pulmonary infiltrates according to X-ray tests (Figure 2).

Throat and anal swabs were obtained from each animal on

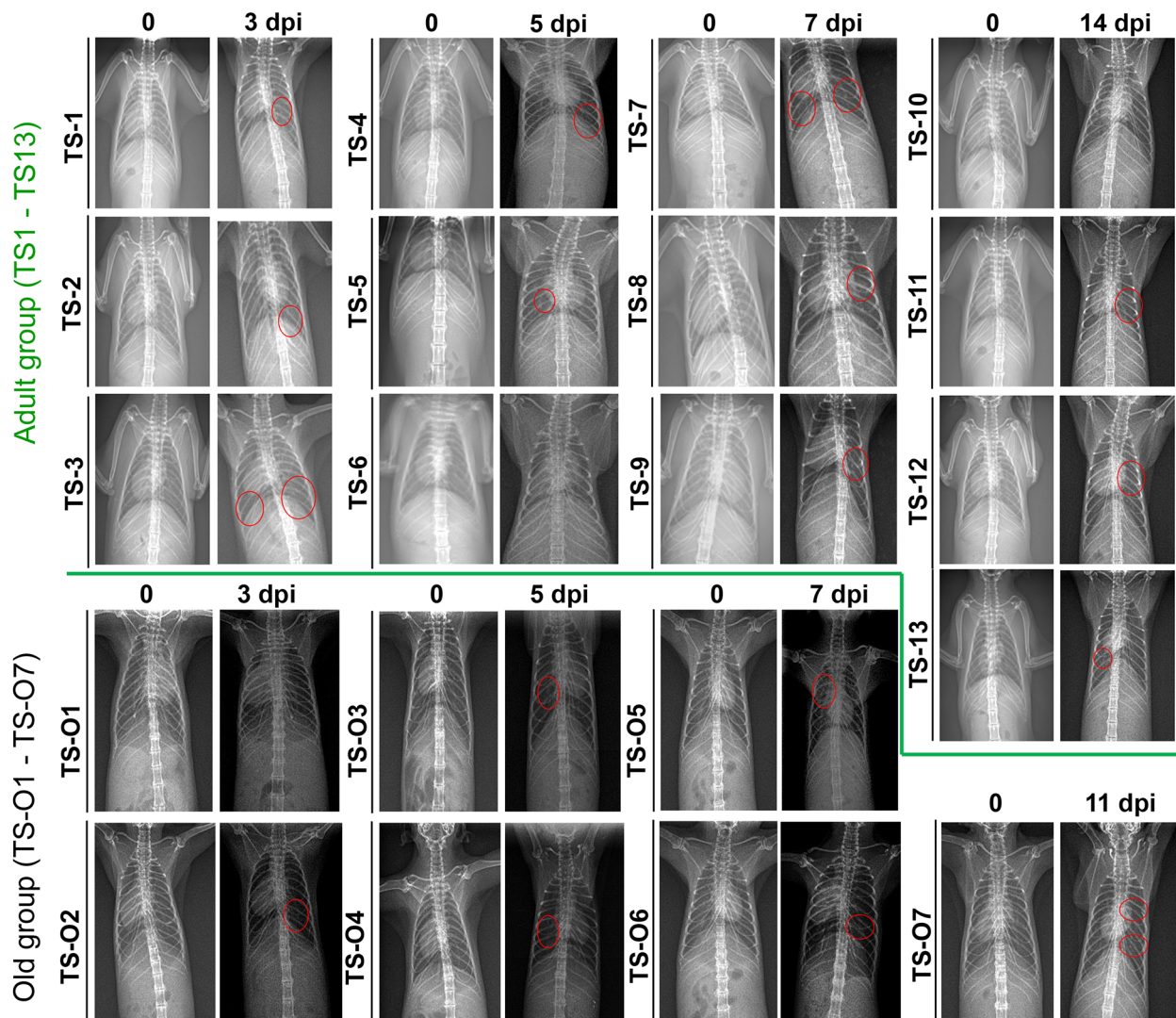


Figure 2 Chest X-rays of tree shrews before and after SARS-CoV-2 inoculation
Circled areas on radiographs are regions showing lung infiltrates.

the days of examination. However, SARS-CoV-2 RNA was undetectable in all swabs from the infected tree shrews. Viral RNA was also undetectable in serum samples of the infected animals (Figure 3A). However, measurement of viral loads in different lobes of the lung and other tissues (conjunctiva, kidney, urinary bladder, small intestines, testes, and ovaries) showed that most lung lobes had higher numbers of viral RNA copies (Figure 3B) in the adult group. For the different examination days, viral RNA in the lung tissue samples peaked at 3 dpi, ranging from 1 360 to 931 777 copies/g, then gradually decreased to undetectable at 14 dpi. In the old group, however, viral RNA was only detected in a few lobes of the lung, with a peak appearing at 7 dpi. Moreover, a low viral copy number was observed in the small intestine (5/20, 25%) and conjunctiva tissues (2/20, 10%) in a small proportion of individuals (Figure 3C). We detected the IgM and neutralizing antibodies in these infected tree shrews but were unable to successfully detect related antibodies (data not shown). Thus, taken together, our results indicate that tree shrews are susceptible to SARS-CoV-2 infection.

We performed histological analysis of lung tissues from animals at 3 dpi in the adult group and 7 dpi in the old group, as these time points showed the highest viral loads in their respective groups. The main gross lesions involved sporadic or massive pulmonary punctate hemorrhage (Figure 4A). Sections of all seven lung lobes showed thickened alveolar septa and interstitial hemorrhage (Figure 4B). Occasionally, alveoli contained small numbers of pulmonary lymphocytes

and neutrophils. Immunofluorescence using a murine antibody against SARS-CoV NP demonstrated the presence of viral antigen in a small number of pneumocytes (Figure 4C).

The overall pattern of laboratory assessments in animals before and after SAR-CoV-2 inoculation (Tables 1, 2) exhibited several features. First, the white blood cell ($P=0.0017$), lymphocyte ($P=0.023$), monocyte ($P=0.0176$), and granulocyte counts ($P=0.0028$) were obviously elevated after infection in the adult group (Table 1). This pattern is different from that of patients with COVID-19, in which lymphocytopenia is common (Guan et al., 2020). However, we did observe a significant decrease in monocytes ($P=0.0009$) in the old group after SARS-CoV infection (Table 2) (Figure 5A). The exact reason for this age-related difference remains to be determined. Second, BUN and albumin were significantly altered in both groups of animals after viral infection. Moreover, there was a marked increase in AST with SARS-CoV-2 infection in the adult group (Figure 5B). These observations reflected impaired liver and renal function, consistent with reported laboratory findings that AST is elevated during COVID-19 progression (Zhang et al., 2020a). Further histological and immunohistochemical analyses and viral detection should be performed on liver and kidney tissues of infected tree shrews to confirm impaired liver and renal function and the presence of viral loads in these organs.

DISCUSSION

The COVID-19 pandemic continues to spread worldwide due

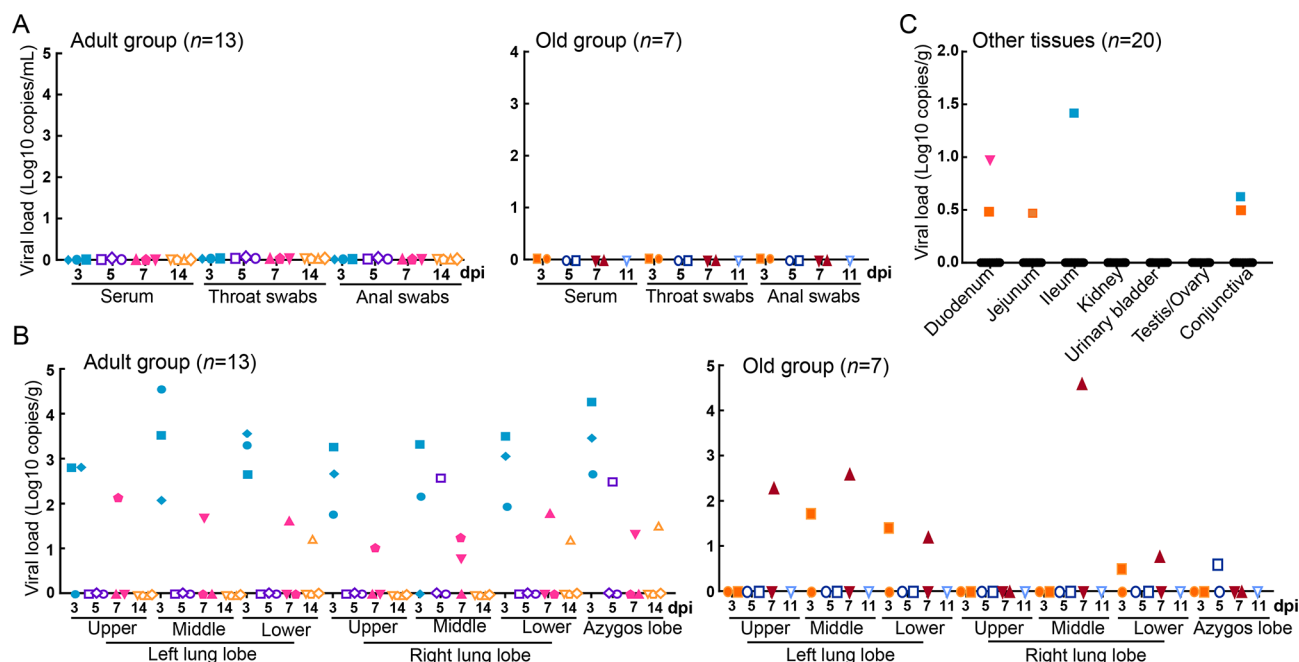


Figure 3 Viral loads of SARS-CoV-2 in Chinese tree shrews

Viral loads in serum and throat/rectal swabs (A), lung lobes (B), and other tissues (C) from infected tree shrews measured using quantitative real-time PCR. Each graphic represents one individual, with color referring to indicated dpi. For instance, three infected animals sacrificed at 3 dpi were defined by square, circle, and diamond, respectively. Marks in blue refer to time point 3 dpi.

to a current lack of approved drugs or vaccines. Recent studies on the infection and transmission of SARS-CoV-2 in different animals have provided new insights into the pathogenesis of SARS-CoV-2 (Bao et al., 2020; Kim et al., 2020; Lu et al., 2020b; Munster et al., 2020; Rockx et al., 2020; Shan et al., 2020; Yu et al., 2020b). Pioneering studies evaluating the clinical benefit of Remdesivir (Williamson et al., 2020) and inactivated vaccine candidate (Gao et al., 2020) in

rhesus macaques infected with SARS-CoV-2 have established a good paradigm for researchers to discover and optimize drug and vaccine candidates for the prevention of SARS-CoV-2 infection and for the treatment of COVID-19. In this study, we found that Chinese tree shrews could be infected with SARS-CoV-2, with consistent detection of viral loads in the lung tissues of infected animals. Compared with available non-human primate models (Lu et al., 2020b; Rockx

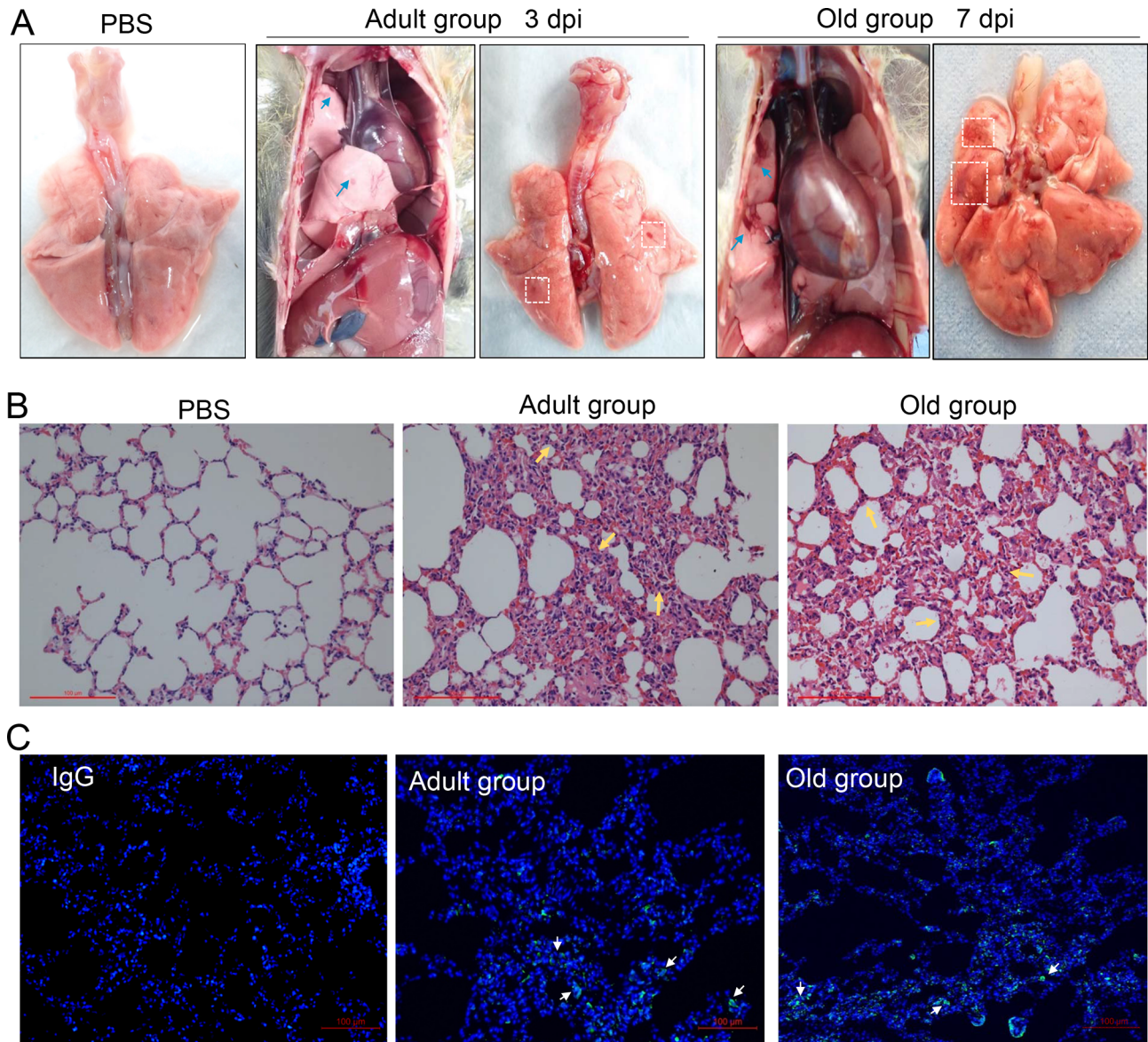


Figure 4 Characterization of lung changes after SARS-CoV-2 infection in Chinese tree shrews

A: Lesions in lungs. Representative view of ventral lungs of infected tree shrew obtained via necropsy at 3 dpi in adult group or at 7dpi in old group compared to healthy control. White box indicates lungs showing focal areas of hyperemia. B, C: Representative hematoxylin and eosin staining (B) and immunofluorescence analysis of viral antigen NP (C) in lung tissues from tree shrews at 3 dpi in adult group or at 7 dpi in old group. Blue arrows in A refer to lesions. Yellow arrows in B indicate pulmonary lymphocytes or neutrophils. White arrows in C indicate SARS-CoV-2 NP staining (green) in pneumocytes, with DAPI staining in blue. PBS and IgG indicate tissue sample from healthy animal in control group treated with PBS but no SARS-CoV-2. Scale bars: 100 μ m.

et al., 2020; Shan et al., 2020; Yu et al., 2020b), the tree shrew model for SARS-CoV-2 infection showed similar lung infiltrates as observed in monkeys and humans. Given their genetic closeness to non-human primates (Fan et al., 2019)

and fewer ethical concerns compared to studies on monkeys, tree shrews are becoming increasingly important in biomedical research. Based on the results in this study, tree shrews may be a valid model for SARS-CoV-2 infection. Certainly, a direct

Table 1 Laboratory findings of adult tree shrews infected with SARS-CoV-2

Parameter	Before inoculation (13/13, 100%)	After inoculation					
		Total (13/13, 100%)	<i>P</i> -value ^a	3 dpi (3/13, 23%)	5 dpi (3/13, 23%)	7 dpi (3/13, 23%)	14 dpi (4/13, 31%)
White blood cell count (×10 ⁹ /L)	1.80±1.12	4.85±3.33	0.0017	1.37±0.70	3.83±1.25	3.77±2.20	8.75±2.62
Lymphocyte count (×10 ⁹ /L)	0.85±0.43	1.34±0.51	0.0230	0.70±0.46	2.27±0.90	1.83±0.71	1.50±0.37
Monocyte count (×10 ⁹ /L)	0.18±0.09	0.38±0.23	0.0176	0.27±0.21	0.47±0.12	0.50±0.44	0.33±0.05
Granulocyte count (×10 ⁹ /L)	0.62±0.46	1.75±1.16	0.0028	0.80±0.70	1.10±0.36	1.43±1.10	3.18±0.14
Lymphocyte percentage (%)	52.64±10.69	51.09±7.86	0.6920	43.90±5.72	59.00±4.15	52.30±10.70	49.65±4.38
Monocyte percentage (%)	13.36±3.92	10.55±4.71	0.1727	14.57±1.17	12.63±3.77	11.67±4.01	5.15±2.63
Granulocyte percentage (%)	34.40±9.02	33.65±7.16	0.9175	41.53±4.56	28.37±2.30	36.03±8.47	29.93±5.07
BUN (mg/dL)	16.46±4.18	23.65±8.43	0.0196	26.00±8.19	23.00±6.25	16.67±11.06	27.50±7.59
TP (g/dL)	6.56±0.28	6.40±0.77	0.4890	5.57±0.38	6.13±0.90	6.87±0.46	6.88±0.57
ALB (g/dL)	3.74±0.44	3.20±0.65	0.0134	2.50±0.26	2.97±0.35	3.60±0.46	3.60±0.71
Globulin (g/dL)	2.82±0.27	3.17±0.26	0.0044	3.07±0.15	3.17±0.55	3.23±0.12	3.20±0.16
ALT (U/L)	151.10±79.21	187.80±123.40	0.2662	141.70±80.59	138.3±77.69	247.70±55.77	214.50±203.40
AST (U/L)	197.00±44.99	467.80±286.20	0.0035	238.30±73.35	583.30±227.00	363.30±75.22	631.50±415.20

^a: *P*-values indicate differences before and after inoculation (total). *P*<0.05 was considered statistically significant. Data are means±SD (Test No./ Total No., %). Paired Student's *t* test. BUN: Blood urea nitrogen, TP: Total protein, ALB: Albumin, ALT: Alanine aminotransferase, AST: Aspartate aminotransferase.

Table 2 Laboratory findings of old tree shrews infected with SARS-CoV-2

Parameter	Before inoculation (7/7, 100%)	After inoculation					
		Total (7/7, 100%)	<i>P</i> -value ^a	3 dpi (2/7, 28%)	5 dpi (2/7, 28%)	7 dpi (2/7, 28%)	14 dpi (1/7, 14%)
White blood cell count (×10 ⁹ /L)	1.45±0.53	3.12±2.25	0.0754	0.80±0.28	6.05±0.49	2.75±1.34	2.90
Lymphocyte count (×10 ⁹ /L)	0.45±0.26	1.67±1.68	0.1101	0.65±0.49	3.2±2.26	1.85±0.21	0.30
Monocyte count (×10 ⁹ /L)	0.21±0.07	0.20±0.16	0.8347	0.05±0.07	0.35±0.21	0.25±0.07	0.10
Granulocyte count (×10 ⁹ /L)	0.77±0.31	1.014±0.95	0.5320	0.50±0.28	0.50±0.28	1.05±0.49	3.00
Lymphocyte percentage (%)	30.77±11.78	46.47±19.90	0.0977	44±8.34	56.80±37.34	51.2±3.11	22.30
Monocyte percentage (%)	16.53±4.19	8.41±2.52	0.0009	8.75±1.62	5.70±2.82	9.10±0.42	11.80
Granulocyte percentage (%)	50.01±7.85	47.23±22.05	0.7583	54.25±16.62	47.9±49.21	39.70±2.68	46.90
BUN (mg/dL)	19.83±5.44	31.29±11.51	0.0087	36.50±6.36	43.00±4.24	21.5±3.53	17.00
TP (g/dL)	6.42±0.36	5.74±0.79	0.0200	5.45±1.06	5.55±0.92	6.50±0.28	5.20
ALB (g/dL)	3.26±0.35	2.50±0.55	0.0017	2.40±0.85	2.35±0.49	2.95±0.49	2.10
Globulin (g/dL)	3.13±0.21	3.25±0.29	0.3080	3.05±0.21	3.2±0.42	3.55±0.21	3.20
ALT (U/L)	202.40±77.66	180.90±122.70	0.6428	187.00±86.27	115.50±33.23	264.50±238.30	132.00
AST (U/L)	229.00±31.97	361.30±316.20	0.1606	192.00±42.43	271.00±183.80	657.50±556.50	288.00

^a: *P*-values indicate differences before and after inoculation (total). *P*<0.05 was considered statistically significant. Data are means±SD (Test No./ Total No., %). Paired Student's *t* test. BUN: Blood urea nitrogen, TP: Total protein, ALB: Albumin, ALT: Alanine aminotransferase, AST: Aspartate aminotransferase.

comparison of the current tree shrew model with other similar-sized animal models commonly used in the laboratory, such as ferrets (Kim et al., 2020; Shi et al., 2020) and golden Syrian hamsters (Chan et al., 2020), could help clarify whether tree shrews are superior to other animal models in mimicking the hallmarks of disease observed from human infection with SARS-CoV-2.

However, there are several limitations regarding the tree shrew model for SARS-CoV-2 infection in this study. First, we did not include juvenile tree shrews, who may be more susceptible to SARS-CoV-2 infection, as age is a risk factor for COVID-19 (Yang et al., 2020) and we did observe differences regarding viral shedding and laboratory tests between adult and old groups. Interestingly, the old tree shrews seemed to be less susceptible to SARS-CoV-2 infection compared with the adult tree shrews based on viral loads in the lung tissues. This pattern is quite different from previous reports, which suggest that SARS-CoV-2 is more virulent in older humans than in younger humans (Guan et al., 2020; Yang et al., 2020). As the sample size of the old group was relatively small, this observation needs to be further validated. Second, we did not provide body temperature data as we could not achieve reliable measurements to confirm whether infected animals had a fever. Other typical symptoms of COVID-19, such as cough, myalgia, dyspnea, fatigue, and headache (Guan et al., 2020), were also not tested due to a lack of related models. Third, we did not characterize cytokine profiling due to a lack of immunological reagents and did not perform detailed analyses of pathological alterations in all tissues of infected animals. The detection of SARS-CoV-2 RNA in intestinal tissues of infected animals deserves further investigation, including histopathological and

immunohistochemical analyses and single-cell RNA sequencing. Similarly, as SARS-CoV-2 is a respiratory pathogen and animals are also infected via this route, analysis of nasal turbinates would also be of benefit to improve knowledge on viral shedding. Fourth, the animals were sacrificed at different time points for lung pathology and viral loads. However, it might be improper to compare different animals sacrificed at different times, particularly as no inbred line of tree shrews is currently available and animals may have a diverse genetic background. Finally, we did not include a group receiving drug treatments, such as Remdesivir or chloroquine, which have been found to inhibit the replication of SARS-CoV-2 in cellular inhibition assays (Wang et al., 2020b), to further evaluate the efficacy of the model for drug tests. Future studies will be carried out to address these needs.

It should be mentioned that during the preparation of our manuscript, we noted a report on SARS-CoV-2 infection in Chinese tree shrews by Zhao and coworkers (Zhao et al., 2020). They used a different procedure compared with ours as they aimed to undertake longitudinal observations of infected animals. Zhao et al. (2020) found no obvious clinical signs in these animals except for an increase in body temperature in some infected tree shrews and mild pulmonary alterations. They could not consistently detect viral shedding at all time points based on nasal, throat, and anal swabs or blood samples. We believe the different procedures used in our study and that of Zhao et al. (2020) may account for the different patterns reported.

In summary, we found that Chinese tree shrews are susceptible to SARS-CoV-2 infection, with lung lesions and alterations in blood biochemical indices observed. Thus, we believe that the Chinese tree shrew infection model could

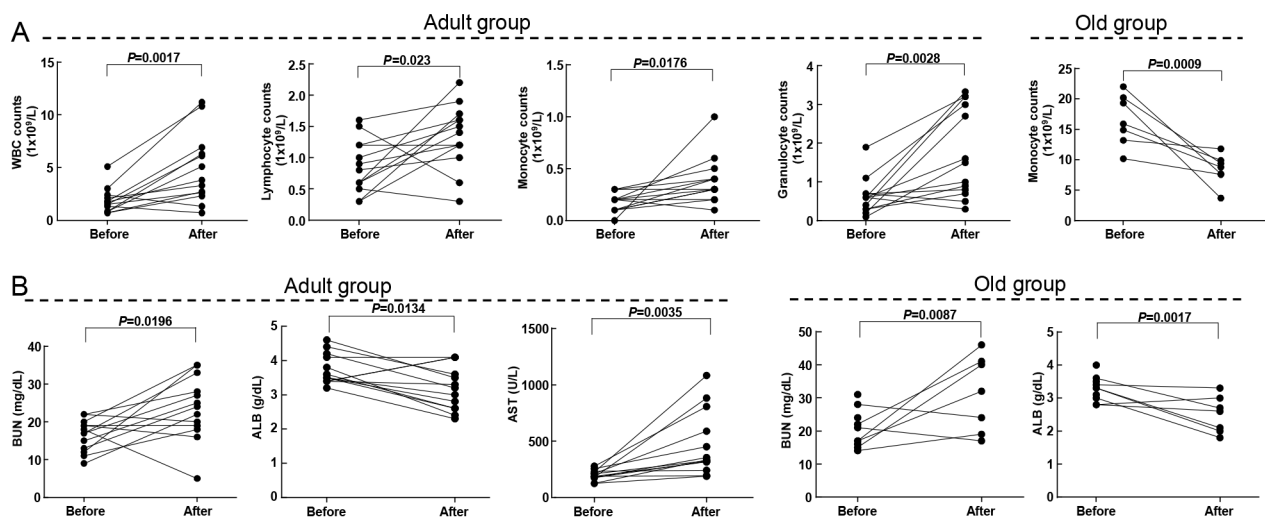


Figure 5 Laboratory findings of altered blood counts (A) and serum biochemistry (B) in tree shrews before and after SARS-CoV-2 infection

Values are means \pm SD. *P*-values were calculated using paired Student's *t* test. Each circle represents one individual, with "Before" and "After" referring to indicated parameter in same animal before SARS-CoV-2 infection and at time of euthanasia, respectively. We grouped all infected animals in each group together, regardless of different infection times of different animals.

potentially be used for drug screening and vaccine evaluation.

COMPETING INTERESTS

The authors declare that they have no competing interests.

AUTHORS' CONTRIBUTIONS

Y.G.Y., Y.T.Z, L.X., and D.D.Y. designed the study and prepared the manuscript. L.X., D.D.Y., Y.H.M., Y.L.Y., R.H.L., X.L.F., J.B.H., X.H.W., and M.H.L. performed the experiments. L.X., D.D.Y., and H.R.C analyzed the data and prepared the figures. C.W.K. provided the virus. All authors read and approved the final version of the manuscript.

ACKNOWLEDGEMENTS

We thank Qi Gen (Primate GLP Safety Assessment Center of the Kunming Institute of Zoology) for technical help with histological analysis and Dr. Gary Wong for helpful comments and language editing. We are very grateful to the two anonymous reviewers for their critical comments on the early version of this manuscript.

REFERENCES

Amako Y, Tsukiyama-Kohara K, Katsume A, Hirata Y, Sekiguchi S, Tobita Y, et al. 2010. Pathogenesis of hepatitis C virus infection in *Tupaia belangeri*. *Journal of Virology*, **84**(1): 303–311.

Bao LL, Deng W, Huang BY, Gao H, Liu JN, Ren LL, et al. 2020. The pathogenicity of SARS-CoV-2 in hACE2 transgenic mice. *Nature*, doi: 10.1038/s41586-020-2312-y.

Chan JFW, Zhang AJ, Yuan SF, Poon VKM, Chan CCS, Lee ACY, et al. 2020. Simulation of the clinical and pathological manifestations of Coronavirus Disease 2019 (COVID-19) in golden Syrian hamster model: implications for disease pathogenesis and transmissibility. *Clinical Infectious Diseases*, doi: 10.1093/cid/ciaa325.

Duan K, Liu BD, Li CS, Zhang HJ, Yu T, Qu JM, et al. 2020. Effectiveness of convalescent plasma therapy in severe COVID-19 patients. *Proceedings of the National Academy of Sciences of the United States of America*, **117**(17): 9490–9496.

Fan Y, Ye MS, Zhang JY, Xu L, Yu DD, Gu TL, et al. 2019. Chromosomal level assembly and population sequencing of the Chinese tree shrew genome. *Zoological Research*, **40**(6): 506–521.

Gao Q, Bao LL, Mao HY, Wang L, Xu KW, Yang M, et al. 2020. Development of an inactivated vaccine candidate for SARS-CoV-2. *Science*, **369**(6499): 77–81.

Geleris J, Sun YF, Platt J, Zucker J, Baldwin M, Hripcsak G, et al. 2020. Observational study of hydroxychloroquine in hospitalized patients with COVID-19. *The New England Journal of Medicine*, **382**(25): 2411–2418.

Goldman JD, Lye DCB, Hui DS, Marks KM, Bruno R, Montejano R, et al. 2020. Remdesivir for 5 or 10 days in patients with severe COVID-19. *The New England Journal of Medicine*, doi: 10.1056/NEJMoa2015301.

Grein J, Ohmagari N, Shin D, Diaz G, Asperges E, Castagna A, et al. 2020. Compassionate use of remdesivir for patients with severe COVID-19. *The New England Journal of Medicine*, **382**(24): 2327–2336.

Guan WJ, Ni ZY, Hu Y, Liang WH, Ou CQ, He JX, et al. 2020. Clinical

characteristics of coronavirus disease 2019 in China. *The New England Journal of Medicine*, **382**(18): 1708–1720.

Kim YI, Kim SG, Kim SM, Kim EH, Park SJ, Yu KM, et al. 2020. Infection and rapid transmission of SARS-CoV-2 in ferrets. *Cell Host Microbe*, **27**(5): 704–709.e2.

Lagier JC, Million M, Gautret P, Colson P, Cortaredona S, Giraud-Gatineau A, et al. 2020. Outcomes of 3, 737 COVID-19 patients treated with hydroxychloroquine/azithromycin and other regimens in Marseille, France: A retrospective analysis. *Travel Medicine and Infectious Disease*, doi: 10.1016/j.tmaid.2020.101791.

Lam TTY, Jia N, Zhang YW, Shum MHH, Jiang JF, Zhu HC, et al. 2020. Identifying SARS-CoV-2-related coronaviruses in Malayan pangolins. *Nature*, doi: 10.1038/s41586-020-2169-0.

Li LH, Li ZR, Wang EL, Yang R, Xiao Y, Han HB, et al. 2016. Herpes simplex virus 1 infection of tree shrews differs from that of mice in the severity of acute infection and viral transcription in the peripheral nervous system. *Journal of Virology*, **90**(2): 790–804.

Li RF, Zanin M, Xia XS, Yang ZF. 2018. The tree shrew as a model for infectious diseases research. *Journal of Thoracic Disease*, **10**(Suppl 19): S2272–S2279.

Lu RJ, Zhao X, Li J, Niu PH, Yang B, Wu HL, et al. 2020a. Genomic characterisation and epidemiology of 2019 novel coronavirus: implications for virus origins and receptor binding. *The Lancet*, **395**(10224): 565–574.

Lu SY, Zhao Y, Yu WH, Yang Y, Gao JH, Wang JB, et al. 2020b. Comparison of SARS-CoV-2 infections among 3 species of non-human primates. *bioRxiv*, doi: 10.1101/2020.04.08.031807.

Million M, Lagier JC, Gautret P, Colson P, Fournier PE, Amrane S, et al. 2020. Early treatment of COVID-19 patients with hydroxychloroquine and azithromycin: A retrospective analysis of 1061 cases in Marseille, France. *Travel Medicine and Infectious Disease*, **35**: 101738.

Munster VJ, Feldmann F, Williamson BN, van Doremalen N, Pérez-Pérez L, Schulz J, et al. 2020. Respiratory disease in rhesus macaques inoculated with SARS-CoV-2. *Nature*, doi: 10.1038/s41586-020-2324-7.

Reed LJ, Muench H. 1938. A simple method of estimating fifty per cent endpoints. *American Journal of Epidemiology*, **27**(3): 493–497.

Rockx B, Kuiken T, Herfst S, Bestebroer T, Lamers MM, Oude Munnink BB, et al. 2020. Comparative pathogenesis of COVID-19, MERS, and SARS in a nonhuman primate model. *Science*, **368**(6494): 1012–1015.

Shan C, Yao YF, Yang XL, Zhou YW, Gao G, Peng Y, et al. 2020. Infection with novel coronavirus (SARS-CoV-2) causes pneumonia in rhesus macaques. *Cell Research*, doi: 10.1038/s41422-020-0364-z.

Shi JZ, Wen Z, Zhong GX, Yang HL, Wang C, Huang BY, et al. 2020. Susceptibility of ferrets, cats, dogs, and other domesticated animals to SARS-coronavirus 2. *Science*, **368**(6494): 1016–1020.

Tang W, Cao ZJ, Han MF, Wang ZY, Chen JW, Sun WJ, et al. 2020. Hydroxychloroquine in patients with mainly mild to moderate coronavirus disease 2019: open label, randomised controlled trial. *BMJ: British Medical Journal*, **369**: m1849.

Wang DW, Hu B, Hu C, Zhu FF, Liu X, Zhang J, et al. 2020a. Clinical characteristics of 138 hospitalized patients with 2019 novel Coronavirus-infected pneumonia in Wuhan, China. *JAMA*, doi: 10.1001/jama.2020.1585.

Wang ML, Cao RY, Zhang LK, Yang XL, Liu J, Xu MY, et al. 2020b. Remdesivir and chloroquine effectively inhibit the recently emerged novel coronavirus (2019-nCoV) in vitro. *Cell Research*, **30**(3): 269–271.

- Wang Q, Schwarzenberger P, Yang F, Zhang JJ, Su JJ, Yang C, et al. 2012. Experimental chronic hepatitis B infection of neonatal tree shrews (*Tupaia belangeri chinensis*): a model to study molecular causes for susceptibility and disease progression to chronic hepatitis in humans. *Virology Journal*, **9**: 170.
- Wang YM, Zhang DY, Du GH, Du RH, Zhao JP, Jin Y, et al. 2020c. Remdesivir in adults with severe COVID-19: a randomised, double-blind, placebo-controlled, multicentre trial. *The Lancet*, **395**(10236): 1569–1578.
- Williamson BN, Feldmann F, Schwarz B, Meade-White K, Porter DP, Schulz J, et al. 2020. Clinical benefit of remdesivir in rhesus macaques infected with SARS-CoV-2. *Nature*, doi: 10.1038/s41586-020-2423-5.
- Wong G, Bi YH, Wang QH, Chen XW, Zhang ZG, Yao YG. 2020. Zoonotic origins of human coronavirus 2019 (HCoV-19/SARS-CoV-2): why is this work important?. *Zoological Research*, **41**(3): 213–219.
- Wu F, Zhao S, Yu B, Chen YM, Wang W, Song ZG, et al. 2020. A new coronavirus associated with human respiratory disease in China. *Nature*, **579**(7798): 265–269.
- Xiao J, Liu R, Chen CS. 2017. Tree shrew (*Tupaia belangeri*) as a novel laboratory disease animal model. *Zoological Research*, **38**(3): 127–137.
- Xiao KP, Zhai JQ, Feng YY, Zhou N, Zhang X, Zou JJ, et al. 2020. Isolation of SARS-CoV-2-related coronavirus from Malayan pangolins. *Nature*, **583**(7815): 286–289.
- Xu S, Li XY, Yang JY, Wang ZX, Jia Y, Han L, et al. 2019. Comparative pathogenicity and transmissibility of pandemic H1N1, avian H5N1, and human H7N9 influenza viruses in tree shrews. *Frontiers in Microbiology*, **10**: 2955.
- Xu XL, Han MF, Li TT, Sun W, Wang DS, Fu BQ, et al. 2020. Effective treatment of severe COVID-19 patients with tocilizumab. *Proceedings of the National Academy of Sciences of the United States of America*, **117**(20): 10970–10975.
- Yang XB, Yu Y, Xu JQ, Shu HQ, Xia JA, Liu H, et al. 2020. Clinical course and outcomes of critically ill patients with SARS-CoV-2 pneumonia in Wuhan, China: a single-centered, retrospective, observational study. *The Lancet Respiratory Medicine*, **8**(5): 475–481.
- Yao YG. 2017. Creating animal models, why not use the Chinese tree shrew (*Tupaia belangeri chinensis*)?. *Zoological Research*, **38**(3): 118–126.
- Yu B, Li CZ, Chen P, Zhou N, Wang LY, Li J, et al. 2020a. Low dose of hydroxychloroquine reduces fatality of critically ill patients with COVID-19. *Science China Life Sciences*, doi: 10.1007/s11427-020-1732-2.
- Yu P, Qi FF, Xu YF, Li FD, Liu PP, Liu JY, et al. 2020b. Age-related rhesus macaque models of COVID-19. *Animal Models and Experimental Medicine*, **3**(1): 93–97.
- Zhang C, Shi L, Wang FS. 2020a. Liver injury in COVID-19: management and challenges. *The Lancet Gastroenterology & Hepatology*, **5**(5): 428–430.
- Zhang MX, Song TZ, Zheng HY, Wang XH, Lu Y, Zhang HD, et al. 2019. Superior intestinal integrity and limited microbial translocation are associated with lower immune activation in SIVmac239-infected northern pig-tailed macaques (*Macaca leonina*). *Zoological Research*, **40**(6): 522–531.
- Zhang T, Wu QF, Zhang ZG. 2020b. Probable pangolin origin of SARS-CoV-2 associated with the COVID-19 outbreak. *Current Biology*, **30**(7): 1346–1351.e2.
- Zhao Y, Wang JB, Kuang DX, Xu JW, Yang ML, Ma CX, et al. 2020. Susceptibility of tree shrew to SARS-CoV-2 infection. *bioRxiv*, doi: 10.1101/2020.04.30.029736.
- Zhou H, Chen X, Hu T, Li J, Song H, Liu YR, et al. 2020a. A novel bat coronavirus closely related to SARS-CoV-2 contains natural insertions at the S1/S2 cleavage site of the spike protein. *Current Biology*, **30**(11): 2196–2203.e3.
- Zhou P, Yang XL, Wang XG, Hu B, Zhang L, Zhang W, et al. 2020b. A pneumonia outbreak associated with a new coronavirus of probable bat origin. *Nature*, **579**(7798): 270–273.
- Zhu N, Zhang DY, Wang WL, Li XW, Yang B, Song JD, et al. 2020. A novel coronavirus from patients with pneumonia in China, 2019. *The New England Journal of Medicine*, **382**(8): 727–733.